Journal of the European Ceramic Society **6** (1990) 227–235

Susceptibility to Agglomeration of Fine PLZT Powders Prepared from Nitrate Solutions

Yoshio Yoshikawa & Kaoru Tsuzuki

College of Engineering, Nihon University, Koriyama, Fukushima 963, Japan

(Received 19 December 1989; revised version received 2 April 1990; accepted 12 April 1990)

Abstract

PLZT powder which has various degrees of agglomeration was prepared from an aqueous nitrate solution by three hydrolysis methods. They were fine, chemically homogeneous and amorphous. Their particle morphologies, however, were very different due to the different physico-chemical precipitation conditions. Addition of hydrogen peroxide, and a liquid–gas interface reaction were the most effective methods for producing a weakly agglomerated powder by hydrolysis.

Unterschiedlich agglomerierte PLZT Pulver wurden durch drei verschiedene Hydrolysier-Verfahren aus einer wässrigen Nitrat-Lösung hergestellt. Sie waren feinkörnig, chemisch homogen und amorph. Aufgrund der unterschiedlichen physikalisch-chemischen Ausfällbedingungen war die Morphologie der Teilchen jedoch sehr unterschiedlich Die Zugabe von Wasserstoffperoxid und die Reaktion an einer flüssig–gasförmigen Grenzfläche waren die erfolgreichsten Methoden, um ein weich agglomeriertes Pulver durch Hydrolyse herzustellen.

On a préparé des poudres de PLZT présentant différents degrés d'agglomération au moyen de trois méthodes d'hydrolyse d'une solution aqueuse de nitrates. Dans tous les cas, les poudres sont fines, amorphes et chimiquement homogènes. Leurs morphologies sont cependant très dépendantes des conditions physico-chimiques de précipitation. L'addition de peroxyde d'hydrogène et une réaction à l'interface liquide–gaz permettent l'obtention de poudres faiblement agglomérées lors de l'hydrolyse.

1 Introduction

Many desired electrical, optical, mechanical and thermal properties of advanced ceramic materials are related to their composition and microstructures. In optical ceramics, it is well known that lanthanum-modified lead zirconate-titanate (PLZT) containing 8 at.% or more La exhibits the highest transparency[1] and that alumina sintered with MgO which inhibits grain growth can be fabricated into transparent ceramic of theoretical density.[2] The grain size dependence of the Curie temperature,[3,4] planar coupling coefficient[4] and quadratic electro-optic coefficient[5] of PLZT ceramics were also reported.

Both hot pressing[1,3,5] and atmosphere sintering[4,6] have been used to fabricate PLZT ceramics. The firing temperature is normally 1200–1300°C. At such a high temperature the composition and microstructure are difficult to control because of the volatility of PbO during firing. On the other hand, we[7] have developed a 'two-stage sintering' method, which can be used to prepare ceramic parts without setting sand or atmosphere powder at 1100–1200°C. Furthermore, sintering is the more preferable method for mass production.

In general, sintering temperatures can be reduced by using sinterable powders, without degrading the properties of ceramics if adequate calcining, forming and sintering processes are applied. Many chemical preparation (CP) methods[5,8–12] have been investigated to produce sinterable powders in recent years. An increasing trend is toward methods which lower the ceramic processing temperature.

In one work,[12] highly reactive powders were prepared from an inorganic-salt precursor which is

Journal of the European Ceramic Society 0955-2219/90/$3.50

less expensive than organic precursors. Whether the raw material is an inorganic or organic salt, the powder prepared by CP methods is often very fine. Consequently, it is less easily processed than powders traditionally produced from oxide mixtures, because of its submicrometer scale. The smaller the particles the greater their tendency to agglomerate during drying and calcination. The agglomeration of particles precludes dense packing and uniform pore size distribution. The degree of uniformity of packing controls the degree of uniformity of the pore diameter which in turn controls the temperature required for sintering to 100% theoretical density.

The present work attempts to prepare weakly agglomerated and sinterable powders from nitrate salts. Characterization of the powders was performed by surface area and density measurements, pore distribution analyses, thermogravimetric analysis (TG), differential thermal analysis (DTA), X-ray diffraction (XRD), and scanning electron microscopy (SEM) observation.

2 Experimental Procedure

2.1 Preparation

A flow diagram of the powder processing methods employed in this investigation is shown in Fig. 1. Raw materials used to prepare an aqueous clear nitrate mixture were $Pb(NO_3)_2$ (guaranteed chemical reagent, Koso Chemical Co. Ltd, Japan), $La(NO_3)_3 . 6H_2O$ (99·99% pure, Koso Chemical Co. Ltd), $ZrO(NO_3)_2 . 2H_2O$ (guaranteed chemical reagent, Kanto Chemical Co. Inc., Japan), and $TiO(NO_3)_2$. These were dissolved in distilled water to produce 0·07 mol PLZT per liter of solution. The titanyl solution was prepared as follows: titanium hydroxide was precipitated by the hydrolysis of

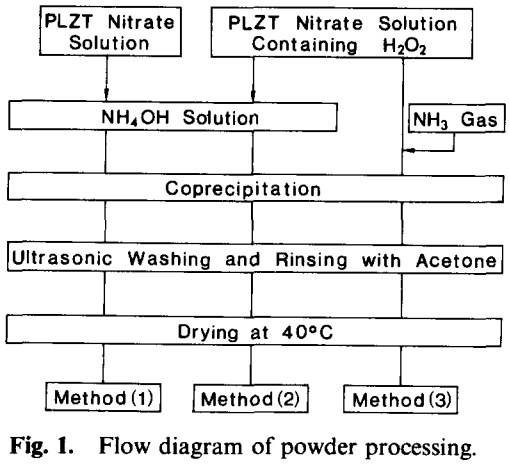

Fig. 1. Flow diagram of powder processing.

$TiCl_4$ (99·999% pure, Koso Chemical Co. Ltd) with an ammonium solution, washed with water to remove Cl^- ions, and redissolved with HNO_3; the concentration of the titanyl solution diluted with distilled water was determined by the gravimetric analysis which involves precipitating titanium hydroxide, igniting at 1000°C and weighing the precipitate of TiO_2. The mixed solution of composition $Pb_{0·92}La_{0·08}(Zr_{0·65}Ti_{0·35})_{0·98}O_3$ (PLZT 8/65/35) was used. The aqueous clear nitrate mixture was hydrolysed by three separate methods.

2.2.1 Method (1)

The aqueous nitrate mixture was added at a rate of 100 ml/min into 15M NH_4OH solution, which was magnetically stirred. Final pH of the solution was about 11·2. Traditional homogeneity considerations when coprecipitating a mixture of four components require that precipitations must be carried out by the reverse strike method. Also, such parameters as pH, concentration and rate of precipitation affect agglomerate, cohesion and size distribution in precipitated powders. Thus care was taken to coprecipitate as homogeneously as possible.

2.2.2 Method (2)

A small amount of hydrogen peroxide was added to the aqueous nitrate mixture before hydrolysis according to the procedure described by Murata *et al.*[9] to improve coprecipitates. The reddish clear nitrate mixture, in which hydrogen peroxide reacts with titanium ions to form peroxotitanium complex ions, was hydrolysed with 15M NH_4OH solution in the same way as Method (1).

2.2.3 Method (3)

The same aqueous reddish nitrate mixture as Method (2) was stirred in a reaction vessel, cooled at 1°C, and was hydrolysed with ammonia gas which was introduced to the liquid surface, with argon carrier gas, for 2 h. The pH of the solution containing the precipitate was monitored with a digital pH meter. Final pH of the solution was 10·5–11·0.

The coprecipitates were then separated from the liquid using a Buchner type porcelain funnel. To provide efficient washing, the filter cake was washed with distilled water and ultrasonically dispersed (45 kHz, 60 W, B2200, Branson, USA) in dilute ammonium solution (pH = 10) for 30 min. The washing and dispersing were repeated twice more. Finally, the cake was ultrasonically rinsed with acetone, and dried at 40°C in an air oven overnight.

2.2 Characterization

The composition of powders was identified by powder X-ray diffraction (Geigerflex 2001, Rigaku Denki Co. Ltd, Japan). 'Drop density' was measured by dropping 10 g of powder from height of 10 cm into a calibrated glass cylinder and then measuring its volume. 'Tap density' was measured next by dropping the cylinder containing the powder from height of 1 cm at a tapping rate of 50 times per minute until the level of powder in the cylinder is unchanged and then measuring its volume. Particle density was measured by a helium-gas pycnometer (Micropycnometer, Quantachrome Co. USA). Particle morphology was observed by SEM (S430, Hitachi Ltd, Japan), and specific surface area was determined by BET method (Quantasorb, Quantachrome). Thermal analysis (TG and DTA) (Thermoflex 8112H, Rigaku Denki Co. Ltd, Japan) was carried out at a heating rate of 10°C/min in air. Nitrogen adsorption and desorption isotherms were measured at its boiling point by the Quantasorb from Quantachrome employing the technique of adsorbing nitrogen gas from a flowing mixture of nitrogen and helium carrier gas. The isotherms obtained with powders (2) and (3) after outgassing as-dried powder and calcined powder at 25°C and 200°C, respectively. The analysis of pore volume distribution was carried out with the aid of a computer. The procedure used is a numerical integration method which takes advantage of Wheeler's theory that condensation occurs in pores when a critical relative pressure is reached corresponding to the Kelvin radius.[13] This method also assumes that an adsorbed multilayer of depth t exists on the pore wall and the Halsey equation can be used for the thickness t in the application.

To investigate the effect of the addition of hydrogen peroxide on the products, a lead nitrate solution (0·05 mol/liter) was hydrolysed with ammonium solution at 25°C in carbon-dioxide-free atmosphere. The precipitate was filtered, washed and dried in a desiccator. The composition of the compound was determined by chemical analysis: the dried product was dissolved in a known amount of dilute nitric acid, filtered and washed with water. The amount of Pb^{2+} in the filtrate was determined by ethylene diaminetetraacetic acid (EDTA) titration using a xylenol orange indicator. The insoluble residue was dissolved completely in a mixture of dilute nitric acid and hydrogen peroxide, and the amount of Pb^{4+} contained in the residue was also determined by EDTA titration.

The effect of atmosphere on crystallization processes during calcination was determined by heating as-dried powders in an atmosphere as follows: the powder (200 mg) was placed in a platinum crucible; the combustion tube containing the crucible was connected to a vacuum line with a gas reservoir of 1000 ml and evacuated to pressure less than $1{\cdot}3 \times 10^{-4}$ atm; oxygen gas was introduced to the vacuum line and the pressure was measured by manometer; nitrogen gas was next introduced to the line until total pressure became 1 atm; the combustion tube was inserted in a furnace controlled within ± 1°C in the sample area; powder was calcined at 415°C and 425°C for 2 h in oxygen partial pressure in the range 0–1·0 atm.

3 Results and Discussion

The precipitate obtained by Method (1) was composed of white flocculates which converted to very hard lumps, which appeared to be with a glassy surface (as-dried powder (1)) during drying (Fig. 2(a,b)). By both Methods (2) and (3) the precipitates were composed of reddish-yellow, fluffy flocculates. When dried, a highly agglomerated particle morphologies (Fig. 2(c,d)) were observed for as-dried powder (2) and a weakly agglomerated particle morphologies (Fig. 2(e,f)) for as-dried powder (3). The lack of sharp images of minimum size agglomerates (about 60 nm) in the micrograph of Fig. 2(e) is a consequence of agglomeration constituting of ultrafine particles, which reduced contrast variations between adjacent agglomerates.

The size and morphology of final precipitates are determined by such processes as nucleation, the growth of primary particles and their agglomeration during hydrolysis reaction. It seems in the case of Methods (3) that nucleation occurs only in the thin layer of liquid–gas interface and that the growth and agglomeration of the nuclei are prevented effectively by stirring the layer. For the liquid–liquid reaction in Method (1) and (2), an extremely large number of nuclei are formed in a moment, with a subsequent agglomeration of these nuclei into gelatinous precipitates.

Both as-dried powders (1) and (2) were free-flowing, while powder (3) tended to stick together or to the surface of containers because of the adhesive surface characteristic of the powder. It is explained by the surface phenomena of fine particles. In general, when the particle size is reduced to 1 μm, Van der Waals attractive force between particles are about six orders of magnitude larger than gravity forces acting on particles.[14] Therefore, the fine particles have a strong tendency to stick as they

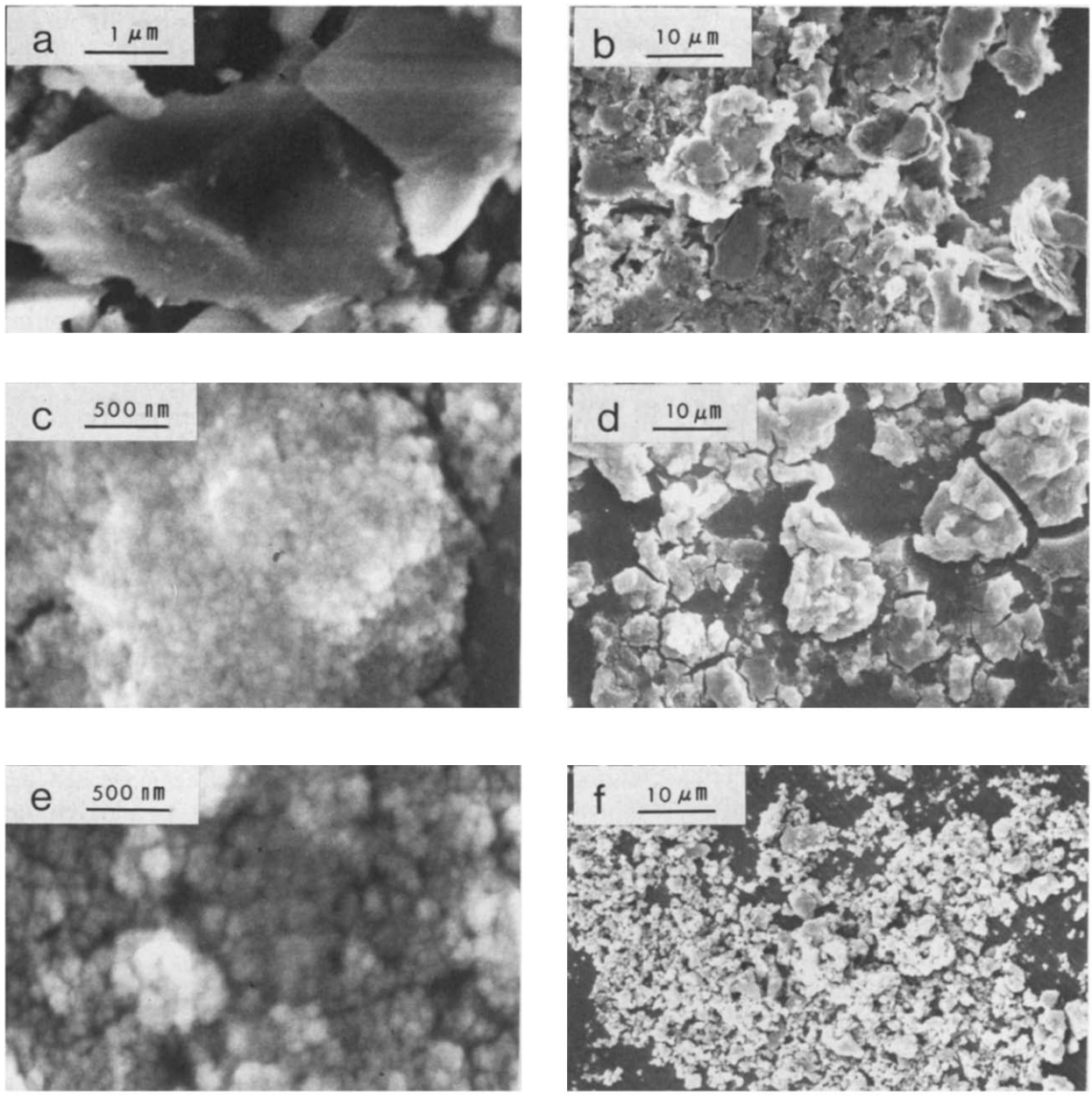

Fig. 2. SEM micrographs of as-dried powder. (a), (b), By Method (1); (c), (d), by Method (2); (e), (f), by Method (3).

come together, with negligible influence of gravity force.

X-ray diffractometry revealed that all precipitates and as-dried powders were amorphous. The colour of as-dried powder (1) was white. On the other hand, the colour of both as-dried powders (2) and (3) was red/yellow, showing a chemical effect of hydrogen peroxide on the coloration. Table 1 gives densities and specific surface areas for the three types of as-dried powders. Apparent particle densities determined by helium gas pycnometer were not influenced by the method of precipitation. 'Drop' and 'tap' densities were, however, greatly influenced. They are complex properties; their value depends on friction forces in the powder and in the case of an agglomerated powder, on the inherent density of agglomerates. Therefore, the greater 'drop' and 'tap' density of the products of Methods (1) and (2) suggests a greater bulk density of the agglomerates.[15] This relation was qualitatively supported by SEM micrographs (Fig. 2). Specific surface area for

Table 1. Characterization of as-dried powders

As-dried powder	*Density* (g/cm^3)			*Specific surface area* (m^2/g)
	By He gas pycnometer	*'Drop'*	*'Tap'*	
Method (1)	4·6	1·01	1·68	84
Method (2)	4·4	0·88	1·36	140
Method (3)	4·4	0·52	0·84	135

Table 2. Effect of hydrogen peroxide on product for $Pb(NO_3)_2$–NH_4OH system

Mole rate $H_2O_2/Pb(NO_3)_2$	*pH*	*Products*	
0	9·5	Crystalline	$Pb_3(NO_3)(OH)_5$[a]
0	11·1	Crystalline	$Pb_3(NO_3)(OH)_5$
1	9·5	Amorphous	$3PbO.2PbO_2.3H_2O$
1	11·1	Amorphous	$3PbO.2PbO_2.3H_2O$
2	9·5	Amorphous	$3PbO.2PbO_2.3H_2O$
2	11·1	Amorphous	$3PbO.2PbO_2.3H_2O$

[a] Identified to 22-659 identification number of the card in *Powder Diffraction File* compiled by the Joint Committee on Powder Diffraction Standards.

powder (1) was lower than that of powders (2) and (3). An increase of surface area for powder (2) was attributed to the chemical effect of hydrogen peroxide. The chemical effects will be described in more detail below.

A previous study[9] described the effects of the addition on the chemical composition and properties of powders as follows: (i) the hydrolysis of the titanium ion was suppressed, (ii) 'lead hydroxide was dehydrated and precipitate which was not the admixture of hydroxides of individual components was yielded', and (iii) 'since part of hydrogen peroxide contained decomposes during drying, the dried cake becomes porous'.

Some results of single component system are presented to illustrate the chemical effect. Table 2 and Fig. 3 show the effect on products for the aqueous lead nitrate solution hydrolysed with ammonium solution. White crystalline precipitates in which a major phase was $Pb_3(NO_3)(OH)_5$ were obtained for the solution in the pH range of 9·5–11·1. When treated with hydrogen peroxide prior to hydrolysis, red/yellow amorphous precipitates were obtained. Hydrogen peroxide oxidised the crystalline lead hydroxide precipitate and converted it into a higher state of oxidation like $3PbO.2PbO_2$. The composition of the red/yellow amorphous

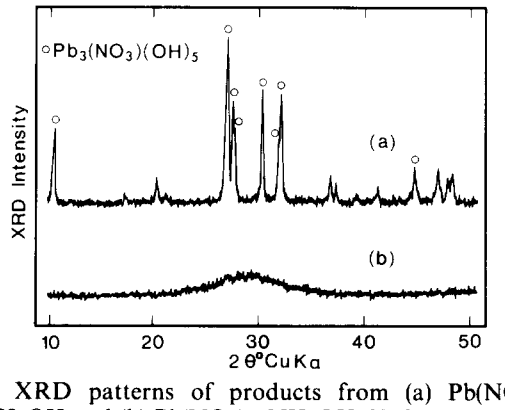

Fig. 3. XRD patterns of products from (a) $Pb(NO_3)_2$–NH_4OH and (b) $Pb(NO_3)_2$–NH_4OH–H_2O_2 system.

products determined by TG and chemical analysis was mainly $3PbO.2PbO_2.3H_2O$. When an aqueous titanium nitrate was hydrolysed with ammonium solution, a white gelatinous compound precipitated and was amorphous by XRD. On the other hand, when treated with hydrogen peroxide and then with ammonium solution, a yellow amorphous precipitate was obtained. TG analysis of the yellow powder dried over concentrated sulfuric acid confirmed that the composition is $TiO_3.H_2O$ (titanium peroxide). The precipitate prepared from the aqueous zirconium nitrate treated with the addition was similar in shape and colour to the precipitate prepared from untreated solution except the former agglomerate size was smaller than the latter size. However, there was quite a difference between their TG–DTA curves, suggesting the possibility of the existence of $Zr(OH)_3OOH$ (hydrated zirconium peroxide).[16] Unfortunately, the composition could not be determined because the lack of reproducibility in weight loss occurred in the range of room temperature to 300°C. In the case of lanthanum, white amorphous precipitates were obtained whether treated with the addition or not, and significant differences in TG–DTA curves and other quality were not found.

As-dried powder (1) was amorphous and did not contain the crystalline $Pb_3(NO_3)(OH)_5$ which was produced in the single component system. Therefore, the coprecipitation prevents the nuclei of lead hydroxide growing to a large cluster alone and mixes the four hydroxides on molecular scale. For the four-components system treated with hydrogen peroxide, a similar homogeneous composition seems to be coprecipitated, and lead, titanium and zirconium peroxide are formed in Methods (2) and (3). The coprecipitates assume a red/yellow colour due to the containing of lead and titanium peroxide components.

Specific surface areas for powders (2) and (3) are higher than that of powder (1) (Table 1). In general, when a gel-like hydroxide (e.g. hydroxide of Ti, Zr, Pb and others) starts to precipitate with the increasing pH of the solution, aggregation of the cations will occur. This process is explained by the formation of polynuclear complexes in which the cations are linked via hydrobridges, or oxobridges.[17] The more the linkage of the bridges develops in hydroxide, the more rigid the precipitate becomes. Besides these bridging hydroxo groups between adjacent cations, cations have non-bridging hydroxo groups and coordinated H_2O depending on its coordination number of the cations. The non-bridging hydroxo groups on particle surface are

removed by interparticle surface condensation reactions during drying, resulting in hard agglomerates.[18] The structure of hydrated lead, titanium and zirconium peroxides are not well-defined, but explanations for the increase of surface area include a reduction of bridge and non-bridging hydroxo groups in coprecipitates.

Ultrasonically rinsing with acetone prior to drying effectively prevented the fine precipitates from forming a strong agglomerate by reducing the capillary forces within the precipitate as a result of lowering the surface tension. The surface tension of acetone is about one third of that of water at 20°C. Preliminary results of a electrophoresis experiment indicate that precipitates are negatively charged in water (pH > 7) and acetone. The electrostatic repulsive forces between particles becomes stronger in low dielectric constant acetone than in water and weakens the agglomeration of particles effectively, if an attractive force is relatively weak (e.g. Van der Waals force). Further, the rinsing removes not only adsorbed water layer on particle surface, but also impurities in the layer which cause hard aggregates by solid bridges. For as-precipitated powder (1) the rinsing with acetone does not extract non-bridging hydroxo groups and the absorbed water effectively, indicating a strong agglomeration state.

Figure 4 illustrates the TG–DTA curves of as-dried powder. The TG curves show the weight loss due to the removal of loosely bonded adsorbed water below 100°C, and trapped acetone (powders (2) and (3)), and dehydration of complex oxy-hydroxide up to 400°C resulting in a weight loss of 13·6, 14·6 and 14·7 wt% for powders (1), (2) and (3), respectively. For powder (1), a small amount of weight loss followed between 400°C and 500°C stepwise. The amount of the loss above 400°C decreased monotonically with increasing the number of washing, indicating the removal of water soluble nitrate impurity[12] which was trapped or occluded among hard agglomerated particles. The DTA curves show one endothermic peak at 110°C, corresponding to the vaporization of water, and two exothermic peaks at 250°C (powders (2) and (3)) and 500°C, respectively. The lower exothermic peak is attributed to the removal of acetone trapped in the network of pores between the ultra-fine particles during rinsing. XRD investigations of samples before and after the exothermic peak at 500°C showed only pseudo-cubic PLZT crystalline phase. Therefore, the exotherm is attributed to the heat of crystallization.[19] For powder (1), no exothermic peak at 250°C shows the difference of chemical affinity between acetone–hydroxide and acetone–hydrate, and at 500°C the exothermic peak of crystallization overlaps with the endothermic peak corresponding to decomposition of nitrate impurity.

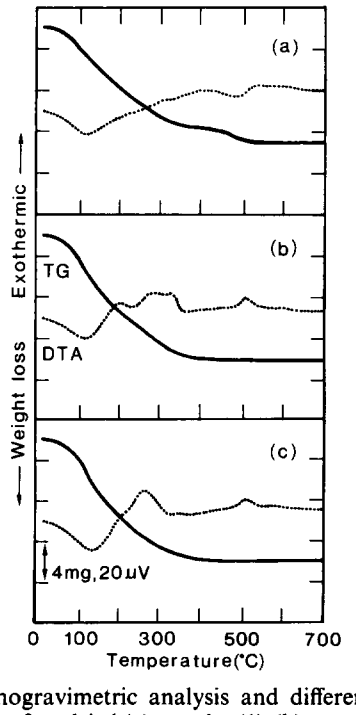

Fig. 4. Thermogravimetric analysis and differential thermal analysis curves of as-dried (a) powder (1), (b) powder (2) and (c) powder (3).

The XRD patterns of the powders were obtained after calcination from room temperature to 700°C. Only pseudo-cubic PLZT phase appeared as low as 400°C, and the intensity of the peak increased with increasing temperature, showing the chemical homogeneity of the coprecipitates. Figure 5 shows the (110) peak of pseudo-cubic PLZT phase on XRD patterns for the powders calcined at 425°C for 2 h in air. The peak of powder (1) is sharp, and both powders (2) and (3) broad. In a previous study,[19] it was shown that powder prepared by Method (3)

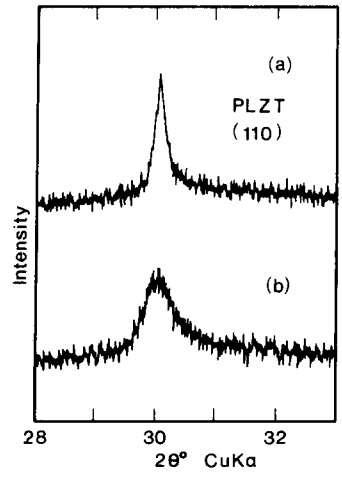

Fig. 5. XRD patterns of (a) powder (1) and (b) powder (3) calcined at 425°C for 2 h.

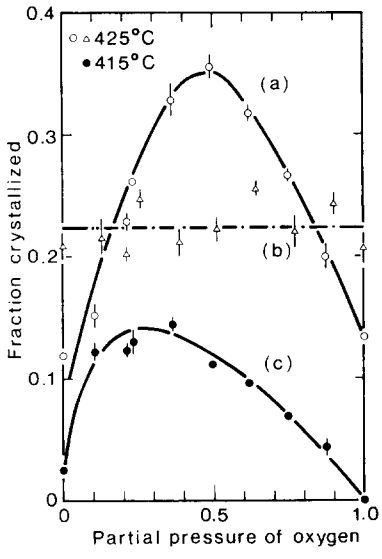

Fig. 6. Fraction crystallized versus partial pressure (atm) of oxygen for: (a), (c) powder (3); (b) powder (1).

consists of 20-nm subunits which agglomerate 60-nm spheres in the temperature range 400–500°C, and that nucleation and growth process are restricted in the subunits of finite size. This restriction does not occur in powder (1) because there is not such a microstructure. Therefore, the sharp peak diffracted from large crystallite could be observed on XRD pattern.

Figure 6 shows the effects of calcination atmosphere and temperature on fraction crystallized. Although data points of powder (1) are scattering, the fraction crystallized is evidently independent of the partial pressure of oxygen. For powder (3), an asymmetrical curved relationship was observed between fraction crystallized and partial pressure of oxygen at 415°C and 425°C. The higher oxide of lead contained in powder (3) will be converted into lead monoxide by heating them to that temperature range. For example, the dissociation pressure for the reaction

$$Pb_3O_4 \rightleftharpoons 3PbO + \tfrac{1}{2}O_2$$

was found.[16] On the chemical equilibrium, large partial pressure of oxygen will suppress the dissociation of higher oxide of lead. Therefore, the smaller the partial pressure, the higher yields of PbO obtained. However, when the partial pressure is lower than the dissociation pressure of the following reaction:

$$PbO \rightleftharpoons Pb + \tfrac{1}{2}O_2$$

lead monoxide is decomposed to metal. The apparent maximum fraction crystallized was taken at the point that the maximum amount of monoxide was attained. It implies that only monoxide of lead

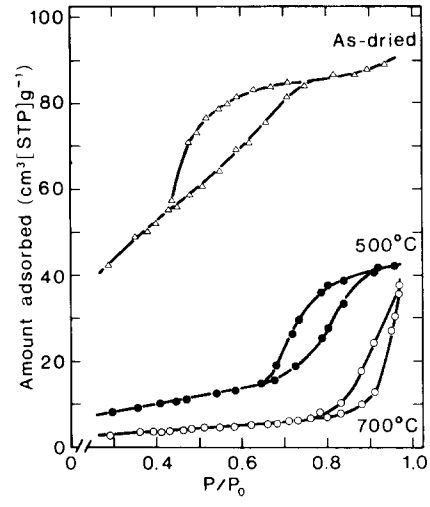

Fig. 7. Nitrogen adsorption–desorption isotherms on powder (2).

can construct the lattice of perovskite structure during heating.

The nitrogen adsorption and desorption isotherms obtained with powders (2) and (3) are illustrated in Figs 7 and 8. The isotherms of powder (2) are of Type A hysteresis[13] reflecting the presence of mesopore. The isotherms of powder (3) seems to be classified to Type II or Type B hysteresis which does not close at the high-pressure end. The difference of amount adsorbed between adsorption and desorption isotherms was small, and amount adsorbed at the saturated pressure could not be determined by the instrument employed. The analysis of pore volume distribution for powder (2) was carried out according to the procedure by Wheeler. Figure 9 shows the distribution curve. The curves indicate that pore radius increases with increasing temperature and that a total pore volume

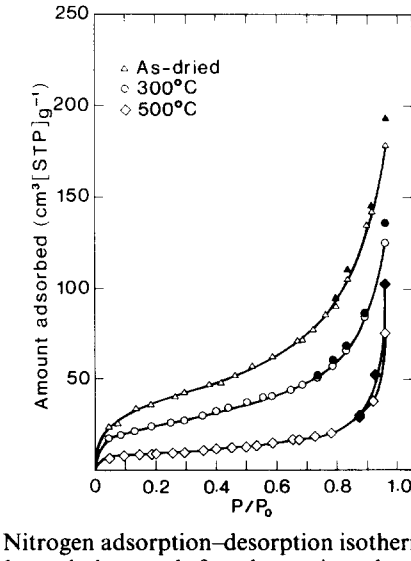

Fig. 8. Nitrogen adsorption–desorption isotherms on powder (3). Solid symbols stand for desorption data points only deviating from adsorption isotherm curve.

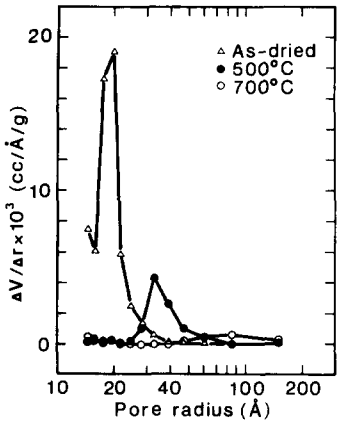

Fig. 9. Pore volume distribution curves of powder (2).

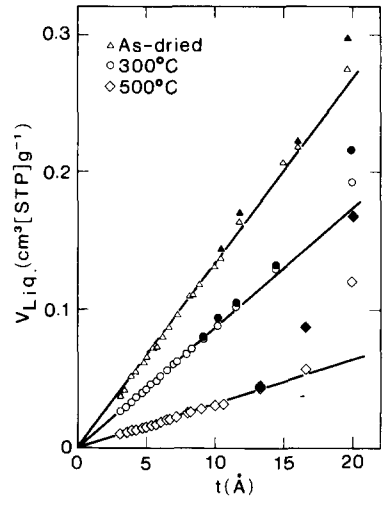

Fig. 10. *V–t* plot for powder (3). Solid symbols stand for desorption data points only deviating from adsorption isotherm curve.

decreases, but not disappear. The existence of broad pore distribution on calcined powders will restrain ceramics from homogeneous densification.

A plot of the volume adsorbed V versus the depth of the adsorbed multi-layer, t, will yield a straight line if condensation of gases into the pore does not take place.[13] Figure 10 illustrates the V_{liq}–t plots, where V_{liq} is the amount of adsorbed nitrogen liquid. All the curves have a straight line in the range of low t-values through the origin. However, above 10 Å upward deviation from the line appears, reflecting the increased uptake due to condensation in larger pores. For powder calcined at 500°C, a hysteresis closed at relative pressure of 0·87 (Fig. 8) appeared due to the pore newly formed among particles by sintering.

4 Conclusions

PLZT powders were prepared from an aqueous nitrate solution by three methods. These were fine, chemically homogeneous and amorphous. Their particle morphologies, however, were very different due to the different physico-chemical co-precipitation conditions. Traditional Method (1) provided fine hydroxide coprecipitates, but they strongly agglomerated during drying. When a small amount of hydrogen peroxide was added prior to hydrolysis, it converted the hydroxide coprecipitates into hydrate oxides and/or hydrate peroxides and seemed to reduce bridge and non-bridging hydroxo groups in coprecipitates. The effect of the addition on powder characteristics such as shape, size and the state of agglomeration are qualitatively explained by the chemistry that the more the linkage of bridge hydroxo group develops in the precipitate, the more rigid the precipitate becomes and that interparticle surface condensation involving non-bridging hydroxo groups is associated with the aggregation of particles during drying. Particle morphologies and related physical characteristics—'drop' density, 'tap' density and adsorption–desorption isotherm—were quite different between Methods (2) and (3). The process of precipitation (nucleation, growth and agglomeration in the solution) markedly affected the state of agglomeration of coprecipitates. Method (3) involving the addition and liquid–gas interface reaction provided the most weak agglomerated powder. The behavior of crystallization and the development of microstructure during calcination were examined as characterization criteria obtaining sinterable powder.

References

1. Haertling, G. & Land, C. H., Hot-pressed (Pb, La)(Zr, Ti)O_3 ferroelectric ceramics for electrooptic applications. *J. Am. Ceram. Soc.*, **54**(1) (1971) 1–11.
2. Bennison, S. J. & Harmer, M. P., Grain-growth kinetics for alumina in the absence of a liquid phase. *J. Am. Ceram. Soc.*, **68**(1) (1985) C22–4.
3. Okazaki, K. & Nagata, K., Effects of grain size and porosity on electrical and optical properties of PLZT ceramics. *J. Am. Ceram. Soc.*, **56**(2) (1973) 82–6.
4. Duran, P. & Moure, C., High density PLZT ceramics prepared chemically from different raw materials. *Am. Ceram. Soc. Bull.*, **64**(4) (1985) 575–9.
5. Song, B.-M., Kim, D.-Y., Yamamura, H., Shirasaki, S. & Tanada, M., Preparation of PLZT ceramics by oxalate method in ethanol solution. *Jpn. J. Appl. Phys.*, suppl. 24–2 (1985) 439–41.
6. Snow, G. S., Fabrication of transparent electrooptic PLZT ceramics by atmosphere sintering. *J. Am. Ceram. Soc.*, **56**(2) (1973) 91–6.
7. Yoshikawa, Y. Tsuzuki, K., Kobayashi, T. & Takagi, A., Chemical preparations and two-stage sintering of PLZT. *Jpn. J. Appl. Phys.*, suppl. 26–2 (1987) 145–8.

8. Brown, L. M. & Mazdiyasni, K. S., Cold-pressing and low-temperature sintering of alkoxy-derived PLZT. *J. Am. Ceram. Soc.*, **55**(11) (1972) 541–4.
9. Murata, M., Wakino, K., Tanaka, K. & Hamakawa, Y., Chemical preparation of PLZT powder from aqueous solution. *Mater. Res. Bull.*, **11** (1976) 323–7.
10. Thomson, J. Jr, Chemical preparation of PLZT powders from aqueous nitrate solutions. *Am. Ceram. Soc. Bull.*, **53**(5) (1974) 421–33.
11. Yoshikawa, Y., Tsuzuki, K., Kobayashi, T. & Takagi, A., Preparation of PLZT powders from several aqueous solutions. *J. Mat. Sci.*, **23** (1988) 2729–34.
12. Yoshikawa, Y. & Tsuzuki, K., The effect of ultrasonic washing on CP-PLZT powder characteristics. In *Proc. MRS Int. Meet. Advanced Materials, Vol. 3*, ed. M. Doyama, S. Somiya & R. P. H. Chang. Materials Research Society, Pittsburgh, PA, 1989, pp. 189–94.
13. Lowell, S. & Shields, J. E., *Powder Surface Area and Porosity*. Chapman and Hall, New York, 1987, pp. 54–74.
14. Rumpt, H. & Schubert, H., *Ceramic Processing before Firing*, ed. G. Y. Onoda Jr & L. L. Hench. John Wiley and Sons, New York, 1978, pp. 357–76.
15. Haberko, K., Characteristics and sintering behaviour of zirconia ultrafine powders. *Ceramurgia International*, **5**(4) (1979) 148–54.
16. Mellor, J. W., *A Comprehensive Treatise on Inorganic and Theoretical Chemistry, Vol. VII*. William Clowes and Sons, London, 1970, pp. 131, 675.
17. Gimblett, F. G. R., *Inorganic Polymer Chemistry*. Butterworths, London, 1963, pp. 77–85.
18. Jones, S. L. & Norman, C. J., Dehydration of hydrous zirconia with methanol. *J. Am. Ceram. Soc.*, **71**(4) (1988) C190–1.
19. Yoshikawa, Y. & Tsuzuki, K., Crystallization of fine, chemically prepared lead lanthanum zirconate titanate powders at low temperature. *J. Am. Ceram. Soc.*, **73**(1) (1990) 31–4.